

The devil is in the details: the role of the radiative corrections

Francesca Dordei, INFN Cagliari

Magnificent CEvNS 2024, 12-14 June 2024 Valencia



francesca.dordei@cern.ch

Momentum dependent flavor radiative corrections to the coherent elastic neutrino-nucleus scattering for the neutrino charge-radius determination

M. Atzori Corona^{a,b}, M. Cadeddu^b, N. Cargioli^{a,b}, F. Dordei^b and C. Giunti^{b,c}

^aDipartimento di Fisica, Università degli Studi di Cagliari,
Complesso Universitario di Monserrato - S.P. per Sestu Km 0.700,
09042 Monserrato (Cagliari), Italy

^bIstituto Nazionale di Fisica Nucleare (INFN), Sezione di Cagliari,
Complesso Universitario di Monserrato - S.P. per Sestu Km 0.700,
09042 Monserrato (Cagliari), Italy

^cIstituto Nazionale di Fisica Nucleare (INFN), Sezione di Torino,
Via P. Giuria 1, I-10125 Torino, Italy

E-mail: mattia.atzori@ca.infn.it, matteo.cadeddu@ca.infn.it,
nicola.cargioli@ca.infn.it, francesca.dordei@cern.ch,
carlo.giunti@to.infn.it

ABSTRACT: Despite being neutral particles, neutrinos can have a non-zero charge radius, which represents the only non-null neutrino electromagnetic property in the standard model theory. Its value can be predicted with high accuracy and its effect is usually accounted for through the definition of a radiative correction affecting the neutrino couplings to electrons and nucleons at low energy, which results effectively in a shift of the weak mixing angle. Interestingly, it introduces a flavour-dependence in the cross-section. Exploiting available neutrino-electron and coherent elastic neutrino-nucleus scattering (CE ν NS) data, there have been many attempts to measure experimentally the neutrino charge radius. Unfortunately, the current precision allows one to only determine constraints on its value. In this work, we discuss how to properly account for the neutrino charge radius in the CE ν NS cross-section including the effects of the non-null momentum-transfer in the neutrino electromagnetic form factor, which have been usually neglected when deriving the aforementioned limits. We apply the formalism discussed to a re-analysis of the COHERENT cesium iodide and argon samples and the NCC-1701 germanium data from the Dresden-II nuclear power plant. We quantify the impact of this correction on the CE ν NS cross-section and we show that, despite being small, it can not be neglected in the analysis of data from future high-precision experiments. Furthermore, this momentum dependence can be exploited to significantly reduce the allowed values for the neutrino charge radius determination.

KEYWORDS: Non-Standard Neutrino Properties, Neutrino Interactions

ARXIV EPRINT: [2402.16709](https://arxiv.org/abs/2402.16709)

BASED ON
JHEP 05 (2024) 271 [ARXIV:2402.16709]

[https://doi.org/10.1007/JHEP05\(2024\)271](https://doi.org/10.1007/JHEP05(2024)271)

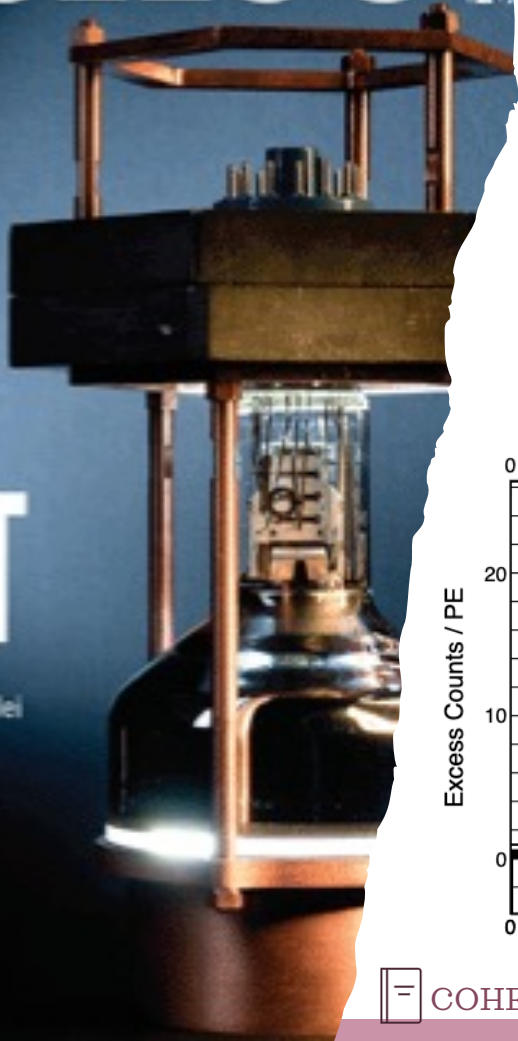


Done in collaboration with: **M. Atzori Corona, M. Cadeddu, N. Cargioli, C. Giunti**

Science

SPOTTING A GHOST

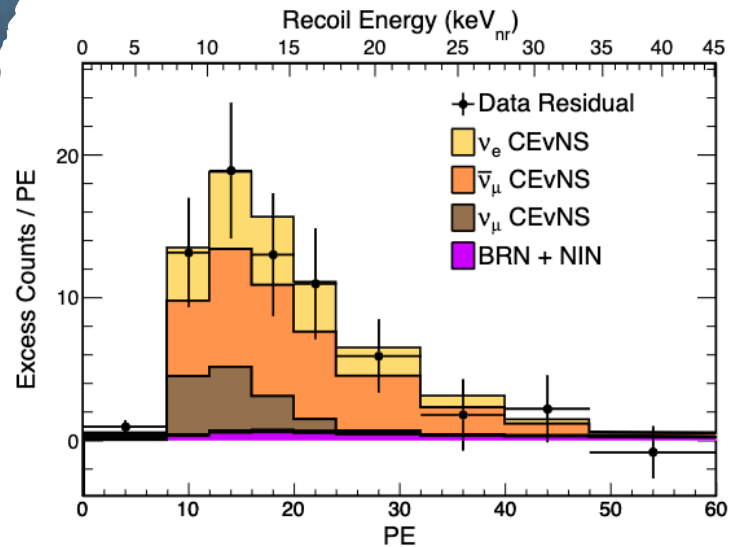
A compact detector spies neutrinos scattering from nuclei pp. 1098 & 1123



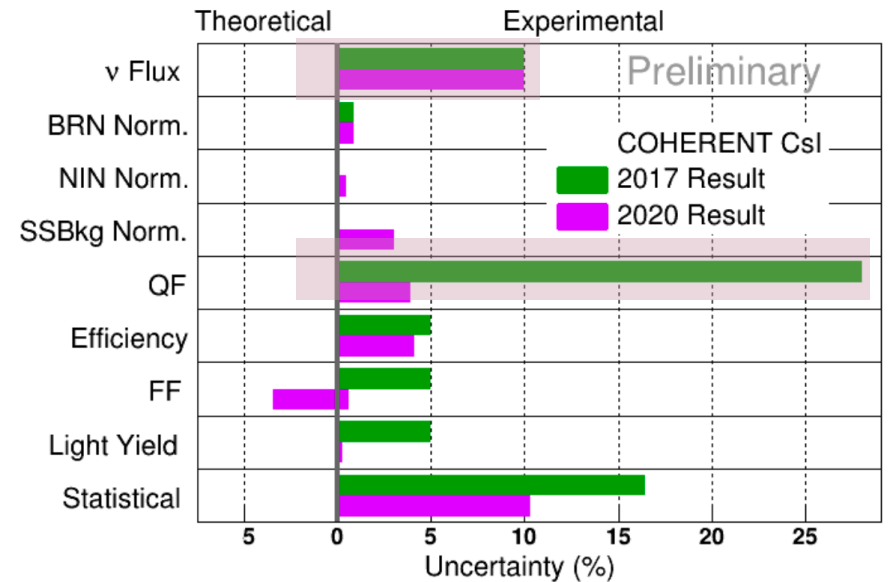
Leading actor I



- Full CEνNS dataset with 14.6 kg CsI scintillating crystal and neutrinos from πDAR
- **306 ± 20 CEνNS** events: 11.6σ significance
- To be compared with prediction: **333±11(th)±42(ex)** events
- ✓ Result is consistent with SM prediction at 1σ
- ✓ Double exposure wrt 2017 and updated quenching factor model
- ✓ Flux uncertainty now dominates the systematic uncertainty.
- ✓ Overall systematic uncertainty reduced: 28% →13%



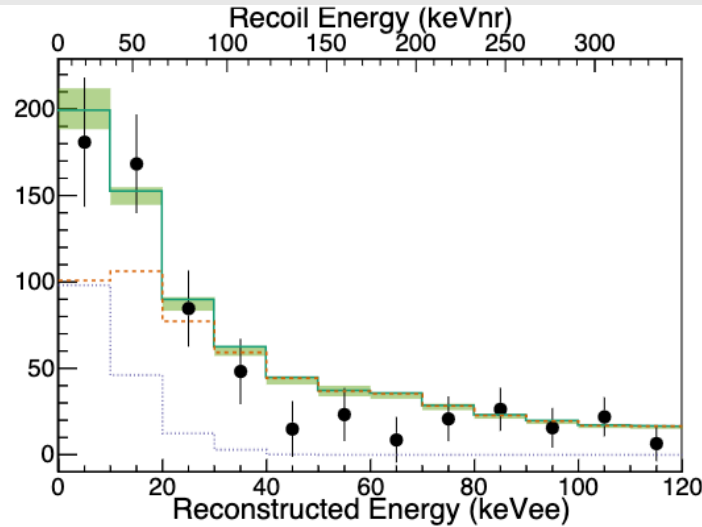
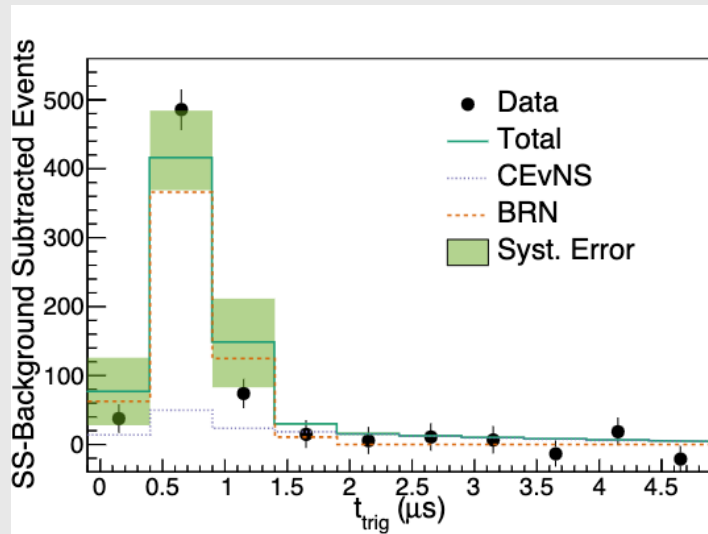
COHERENT, PRL 129, 081801 (2022)



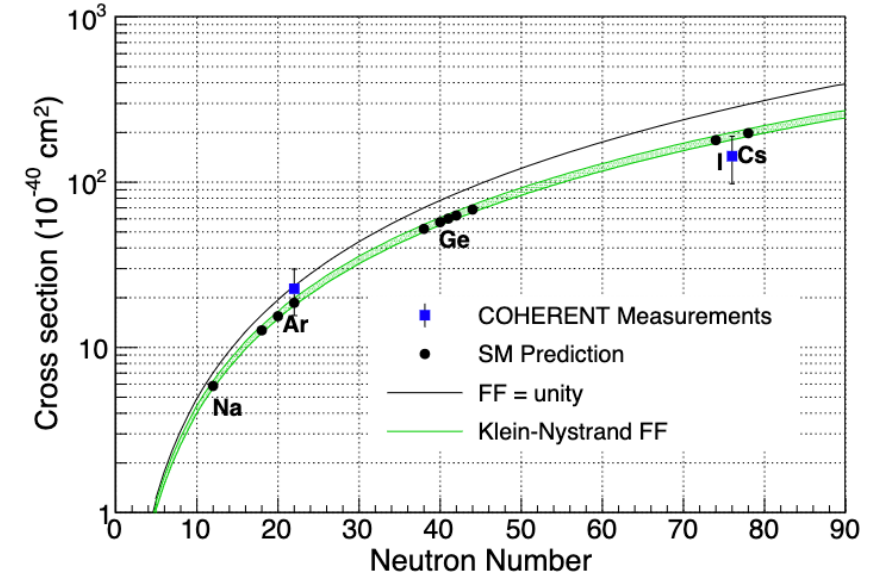
Leading actor II



- 2020 first results using Ar, aka CENNS-10.
- Active mass of 24 kg of atmospheric argon
- Single phase only (scintillation), thr. ~ 20 keV_{nr}
- ✓ Two independent analyses observed a more than 3σ excess over background
- ✓ Still collecting data, more precise results expected soon.



Verify the **expected neutron-number dependence** of cross-section



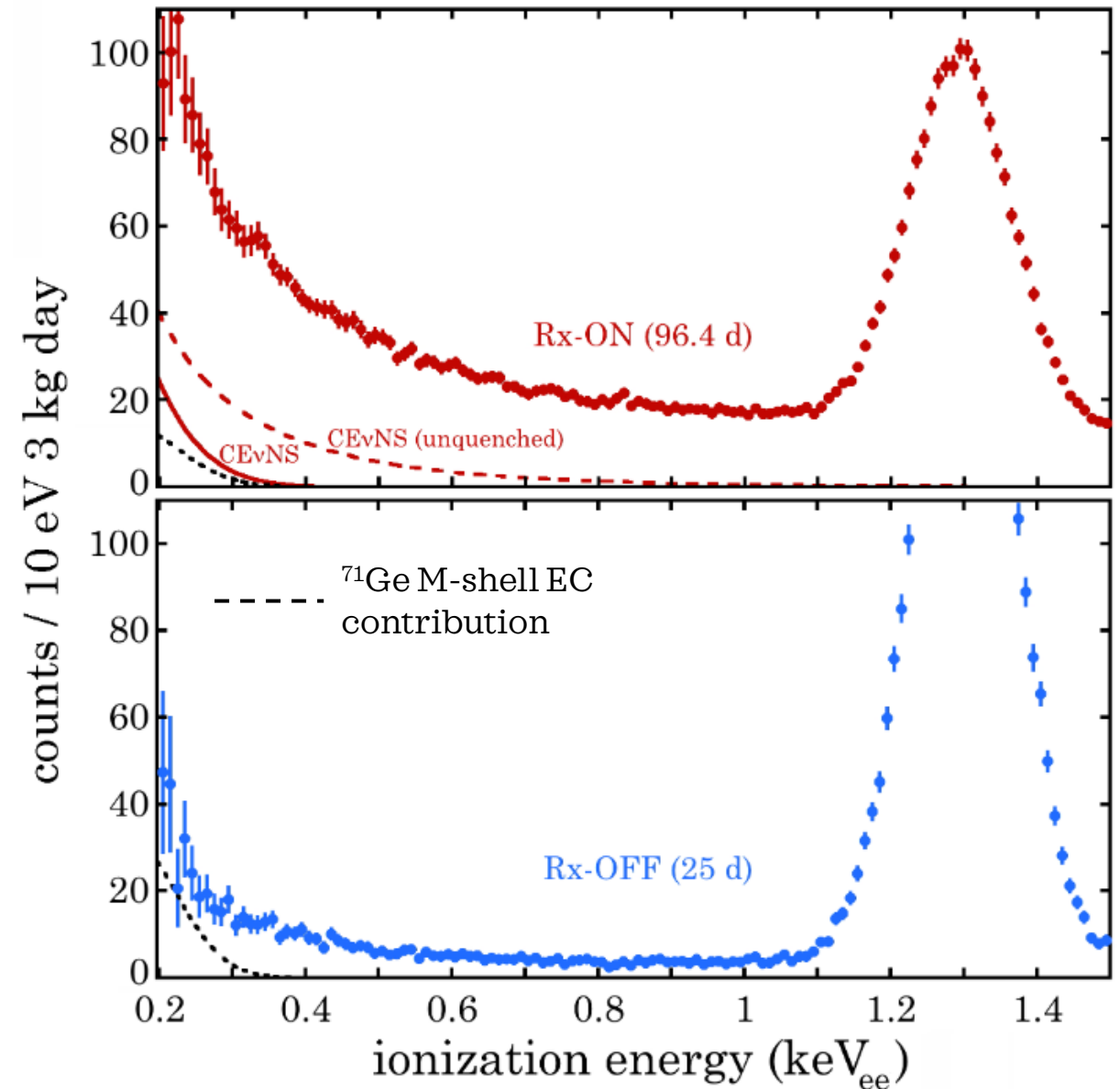
The form factor unity assumption is compared to the Klein-Nystrand parameterization that is used for this analysis with the green band representing a $\pm 3\%$ variation on the neutron radius.

 COHERENT, PRL 126, 012002 (2021)

Leading actor III



- 96.4 day (Rx-ON) exposure of a 3 kg ultra-low noise germanium detector (NCC-1701)
 - 10.39 m away from the Dresden-II boiling water reactor (P=2.96GW_{th})
 - **Low energy threshold:** 0.2 keV_{ee}
 - 25 days of reactor off (Rx-OFF)
 - The background comes from the elastic scattering of **epithermal neutrons** and the **electron capture in ⁷¹Ge**
- $$\frac{dN^{\text{bkg}}}{dT_e} = \underbrace{N_{\text{epith}} + A_{\text{epith}} e^{-T_e/T_{\text{epith}}}}_{\text{epithermal neutrons}} + \underbrace{\sum_{i=L1,L2,M} \frac{A_i}{\sqrt{2\pi}\sigma_i} e^{-\frac{(T_e-T_i)^2}{2\sigma_i^2}}}_{\text{electron capture in } ^{71}\text{Ge}}$$
- **Strong preference** (p<1.2x10⁻³) for the presence of CEνNS is found, when compared to a background-only model.

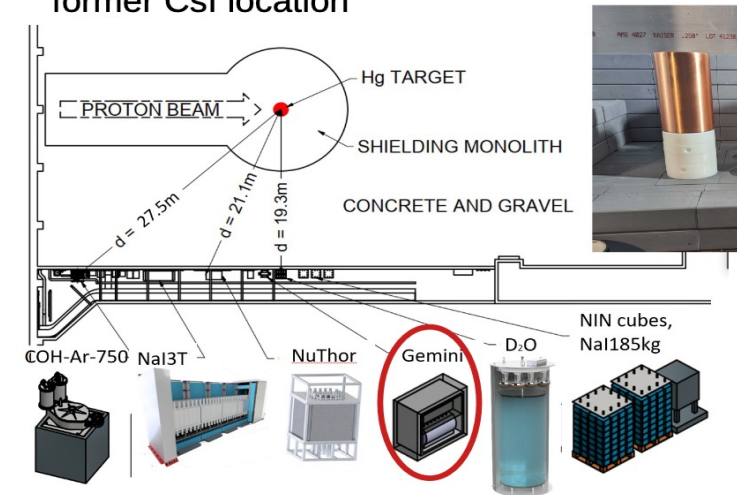


Many other results in the pipeline or expected soon...

- The first measurement of $CE\nu NS$ events on Germanium by COHERENT with the Ge-Mini detector *See R. Bouabid talk!*
- SNS neutrino flux uncertainty reduction from 10% to 2-3% in 5 years thanks to D_2O at the neutrino alley, upgrade of the SNS (higher beam power and energy)
- **NaIvETe**: $CE\nu NS$ on lighter nucleus Na, **COH-Ar-10** with 3 times more statistics and **CO-Ar-750** (ton scale), **COH-CryoCsI** with a significantly lower threshold (~ 0.5 KeVnr), ...

Ge-Mini

distance to target: **(19.1 \pm 0.1)m**
former CsI location



J. Hakenmueller, [JEPT Seminar](#)

Plethora of other experiments expecting to detect $CE\nu NS$ soon!

Just looking at the agenda of Mag7's 2024: CONUS(+), NUCLEUS, MINER, ν GEN, RED-100, CONNIE, RICOCHET, NEON, $CE\nu NS$ @ ESS, Dark Matter experiments...

Soon, we can not afford to be sloppy anymore since we will reach the precision frontier!

LET'S HAVE A CLOSER LOOK TO THE INGREDIENTS NEEDED

$$\frac{d\sigma^{CE\nu NS}(E_\nu, T_{nr})}{dT_{nr}} \cong \frac{G_F^2 m_N}{\pi} \left(1 - \frac{m_N T_{nr}}{2E_\nu^2}\right) \left[g_V^p(\sin^2(\vartheta_W)) Z F_Z(|\vec{q}|^2) + g_V^n N F_N(|\vec{q}|^2) \right]^2$$

Neutrino energy \swarrow E_ν Mass of the nucleus \downarrow m_N SM vector proton coupling \downarrow g_V^p SM vector neutron coupling \downarrow g_V^n
 \uparrow T_{nr} \uparrow T_{nr} \uparrow $\sin^2(\vartheta_W)$ \uparrow $Z F_Z(|\vec{q}|^2)$ \uparrow $N F_N(|\vec{q}|^2)$
 Nuclear recoil energy Weinberg angle Proton Form Factor Neutron Form Factor



At **tree-level** the CE ν NS process is completely flavour-blind and the **SM vector couplings** are:

$$g_V^p(\nu_{e,\mu,\tau}) = \frac{1}{2} - 2\sin^2\vartheta_W \cong 0.0227$$

$$g_V^n(\nu_{e,\mu,\tau}) = -\frac{1}{2} = -0.5$$

Using $\sin^2\vartheta_W(q^2 \approx 0) = 0.23863(5)$

BEYOND TREE LEVEL

At increasing precision, one needs to consider **radiative corrections** due to higher-order vertex contributions.

- In Erler & Su, a strategy is proposed **for EW processes** to calculate most of these corrections in a **universal** way that is **valid at all orders**.

See the RGE formalism in Erler & Su, arXiv 1303.5522 (2013)

- For neutral current processes, the corrections are **absorbed in the definitions of the low-energy EW couplings**

$$g_V^p \text{ and } g_V^n$$

- **Remaining smaller corrections are assumed to be applied individually for each experiment.**, i.e. EW coupling parameters are defined at some common reference scale μ (they choose $\mu = 0$), and have the experimental collaborations correct for effects due to $q^2 \neq 0$.



Overlooked for CE ν NS experiments so far.



NEED TO GO BEYOND TREE LEVEL

When including the **UNIVERSAL radiative corrections** the couplings become:

$$g_V^p(\nu_\ell) = \rho \left(\frac{1}{2} - 2 \sin^2 \vartheta_W \right) + 2\boxtimes_{WW} + \square_{WW} - 2\phi_{\nu_\ell W} + \rho(2\boxtimes_{ZZ}^{uL} + \boxtimes_{ZZ}^{dL} - 2\boxtimes_{ZZ}^{uR} - \boxtimes_{ZZ}^{dR})$$

$$g_V^n = -\frac{\rho}{2} + 2\square_{WW} + \boxtimes_{WW} + \rho(2\boxtimes_{ZZ}^{dL} + \boxtimes_{ZZ}^{uL} - 2\boxtimes_{ZZ}^{dR} - \boxtimes_{ZZ}^{uR}).$$

Following the RGE formalism in Erler & Su, arXiv 1303.5522 (2013) as used in the PDG.

Where $\rho=1.00063$ represents a low-energy correction for neutral current processes and:

WW box $\square_{WW} = -\frac{\hat{\alpha}_Z}{2\pi\hat{s}_Z^2} \left[1 - \frac{\hat{\alpha}_s(M_W)}{2\pi} \right]$ **WW crossed-box** $\boxtimes_{WW} = \frac{\hat{\alpha}_Z}{8\pi\hat{s}_Z^2} \left[1 + \frac{\hat{\alpha}_s(M_W)}{\pi} \right]$

$\boxtimes_{ZZ}^{fX} = -\frac{3\hat{\alpha}_Z}{8\pi\hat{s}_Z^2\hat{c}_Z^2} (g_{LX}^{\nu_\ell f})^2 \left[1 - \frac{\hat{\alpha}_s(M_Z)}{\pi} \right]$ **ZZ box**

while the remaining radiative term is related to the so-called **neutrino charge radius**

$$\phi_{\nu_\ell W} = -\frac{\alpha}{6\pi} \left(\ln \frac{M_W^2}{m_\ell^2} + \frac{3}{2} \right)$$

Up to 67% difference wrt tree-level

In this scenario, **the couplings become flavour-dependent and different from tree-level:**

$$g_V^p(\nu_e) \simeq 0.0381$$

$$g_V^p(\nu_\mu) \simeq 0.0299$$

$$g_V^p(\nu_\tau) \simeq 0.0255$$

$$g_V^n \simeq -0.5117$$



A hand holding a magnifying glass over a city street at night, with bokeh lights in the background. The magnifying glass is positioned over a circular inset showing a busy city street with many neon signs and buildings. The background is filled with out-of-focus, colorful bokeh lights in shades of yellow, orange, blue, and pink.

NEUTRINO CHARGE RADII

Neutrino charge radius - definition

- In the SM, the neutrino charge radii (CR) are the **only electromagnetic properties of neutrinos that are different from zero**.
- A neutral particle can be seen as the superposition of two charge distributions of opposite signs described by an **electric form factor** which is nonzero only for momentum transfers q^2 different from zero

$$f_Q(q^2) = f_Q(0) + q^2 \frac{df_Q(q^2)}{dq^2} \Big|_{q^2=0} + \dots$$

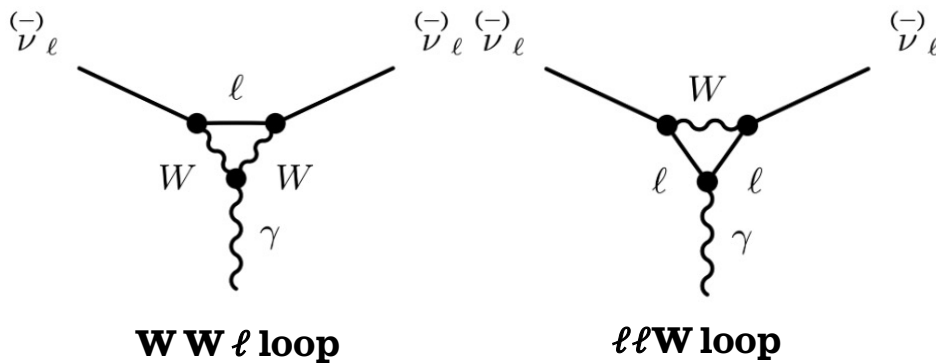
=0 since ν s are neutral

$$\langle r^2 \rangle \equiv 6 \frac{df_Q(q^2)}{dq^2} \Big|_{q^2=0}$$

Neutrino charge radius

i.e. the radius of the electric charge distribution

The charge radius is generated by a **loop insertion into the ν_ℓ line**, where W boson and charged lepton ℓ can enter:



The **NCR is a physical observable**, being finite and gauge invariant!

Bernabeu et al, Phys.Rev.D62:113012 (2000)

$$\langle r_{\nu_\ell}^2 \rangle_{\text{SM}} = -\frac{G_F}{2\sqrt{2}\pi^2} \left[\underbrace{3}_{\text{WW}\ell \text{ loop}} - 2 \ln \left(\frac{m_\ell^2}{m_W^2} \right) \right]_{\ell\ell W \text{ loop}}$$

The $\ell\ell W$ loop introduces a **dependence of the neutrino CR from the lepton flavour**:

$$\begin{aligned} \langle r_{\nu_e}^2 \rangle &\simeq -8.3 \times 10^{-33} \text{ cm}^2 \\ \langle r_{\nu_\mu}^2 \rangle &\simeq -4.8 \times 10^{-33} \text{ cm}^2 \\ \langle r_{\nu_\tau}^2 \rangle &\simeq -3.0 \times 10^{-33} \text{ cm}^2 \end{aligned}$$

Neutrino charge radius – practically speaking

- The neutrino CR affects the scattering of neutrinos with charged particles.
- In the case of CEvNS **it contributes only to the neutrino-proton coupling**, and not to the neutron one.

CEvNS case:

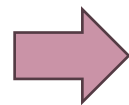
$$g_V^p \rightarrow \tilde{g}_V^p - \frac{2}{3} M_W^2 \langle r_{\nu_\ell}^2 \rangle \sin^2 \vartheta_W = \tilde{g}_V^p - \frac{\sqrt{2}\pi\alpha}{3G_F} \langle r_{\nu_\ell}^2 \rangle$$

Effective shift of the weak mixing angle

$\tilde{g}_V^p \simeq 0.0184$ ν -proton coupling without the contribution of the SM CR

with $\langle r_{\nu_\ell}^2 \rangle_{\text{SM}} = -\frac{G_F}{2\sqrt{2}\pi^2} \left[3 - 2 \ln \left(\frac{m_\ell^2}{m_W^2} \right) \right]$

- Interesting quantity to measure, as **new particles entering the loops could modify it!**
- So far, **only constraints** have been put on its value
- However, keep in mind that the neutrino charge radius is defined at $q^2 \equiv 0$, while **none of the experiments is performed at null-momentum transfer!**



Must be taken into account when implementing radiative corrections in CEvNS processes and when measuring the ν charge radius!

How to deal with non-null momentum transfers?

- Look at **process - dependent radiative corrections** defined by Marciano et al. in arXiv:0403168.

$$\sin^2 \vartheta_W(q^2) = k_{\nu_\ell}(q^2) \sin^2 \vartheta_W(M_Z)$$

where for **neutrino scattering**:

$$k_{\nu_\ell}(q^2) = 1 - \frac{\alpha}{2\pi\hat{s}_Z^2} \left[2 \sum_f (T_{3f} Q_f - 2\hat{s}_Z^2 Q_f^2) J_f(q^2) + \frac{\hat{c}_Z^2}{3} + \frac{1}{\hat{c}_Z^2} \left(\frac{19}{8} + \frac{17}{4} \hat{s}_Z^2 + 3\hat{s}_Z^4 \right) - \left(\frac{7}{2} \hat{c}_Z^2 + \frac{1}{12} \right) \ln \hat{c}_Z^2 \right] \boxed{-\frac{\alpha}{\pi\hat{s}_Z^2} \left[-R_\ell(q^2) + \frac{1}{4} \right]},$$

with:
 $R_\ell(0) = \frac{1}{6} \ln \frac{m_\ell^2}{M_W^2}$
 $R_\ell(q^2) = \int_0^1 dx x(1-x) \ln \left[\frac{m_\ell^2 - q^2 x(1-x)}{M_W^2} \right]$

For $q^2 \rightarrow 0$ we retrieve the same radiative correction as in the RGE formalism:

RGE $\boxed{\phi_{\nu_\ell W} = -\frac{\alpha}{6\pi} \left(\ln \frac{M_W^2}{m_\ell^2} + \frac{3}{2} \right)}$

$$\boxed{\phi_{\nu_\ell W} = -\frac{\alpha}{\pi} \left(-R_\ell(0) + \frac{1}{4} \right)}$$

with a clear advantage:

$$\begin{aligned} \phi_{\nu_\ell W}^{\text{eff}}(q^2) &= -\frac{\alpha}{\pi} \left(-R_\ell(q^2) + \frac{1}{4} \right) \\ &= -\frac{\alpha}{\pi} \left(-\int_0^1 dx x(1-x) \ln \left[\frac{m_\ell^2 - q^2 x(1-x)}{M_W^2} \right] + \frac{1}{4} \right) \end{aligned}$$

The radiative correction includes the momentum dependence!

The effective charge radius form factor

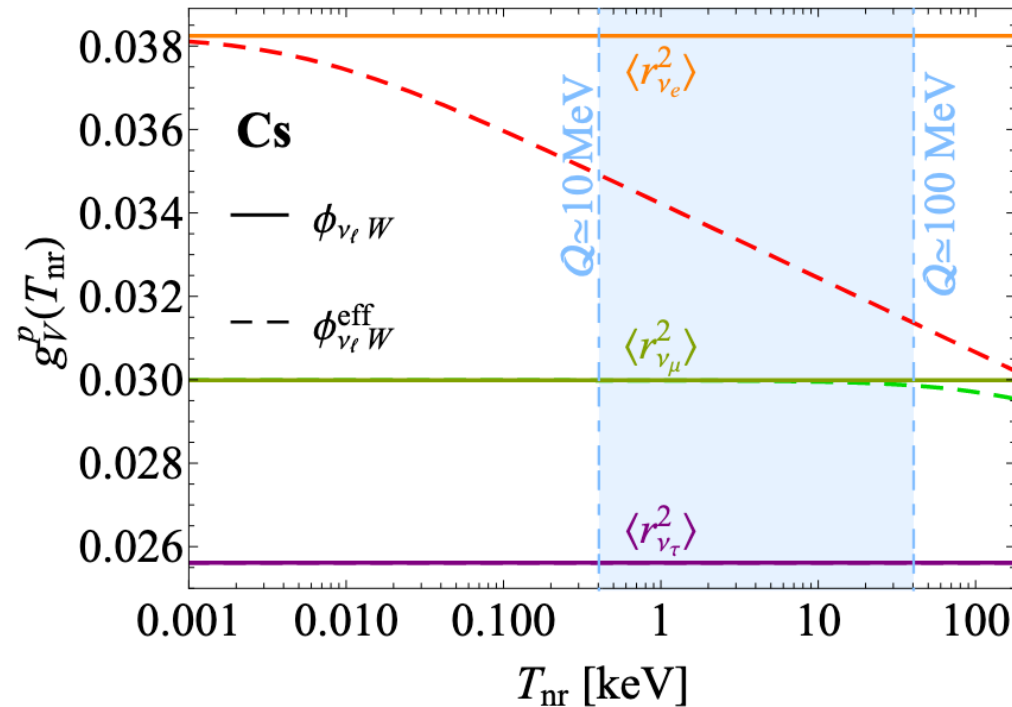
We introduce a **neutrino charge radius form factor** $\mathcal{F}_{\nu_\ell}(T_{\text{nr}}) = \frac{\langle r_{\nu_\ell}^2 \rangle^{\text{eff}}(T_{\text{nr}})}{\langle r_{\nu_\ell}^2 \rangle^{\text{eff}}(0)} \equiv \frac{\langle r_{\nu_\ell}^2 \rangle^{\text{eff}}(T_{\text{nr}})}{\langle r_{\nu_\ell}^2 \rangle^{\text{SM}}}$

with $\langle r_{\nu_\ell}^2 \rangle^{\text{eff}} = \frac{6G_F}{\sqrt{2}\pi\alpha} \phi_{\nu_\ell W}^{\text{eff}}(q^2) = -\frac{G_F}{2\sqrt{2}\pi^2} [3 - 12R_\ell(q^2)]$

From which we obtain an updated proton coupling:

Impact visible for $q^2 \gtrsim m_\ell^2$:

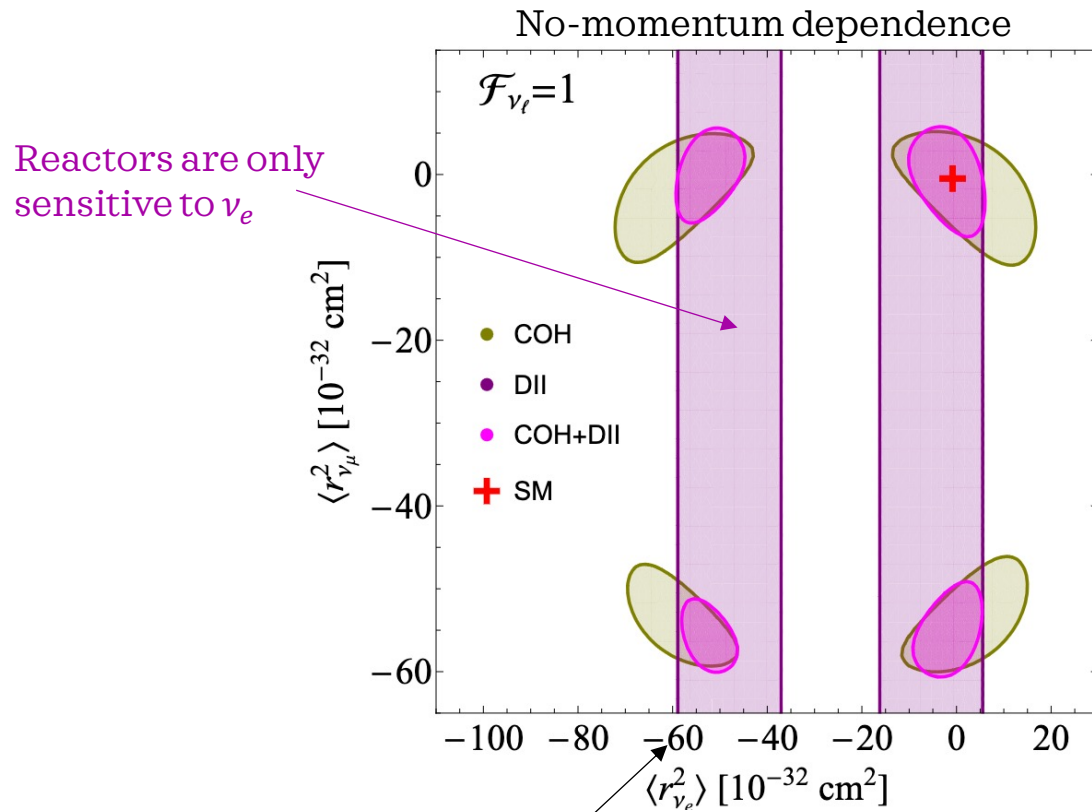
- for ν_e processes the correction becomes visible for $q \gtrsim 0.5$ MeV
- for ν_μ only above ~ 100 MeV!



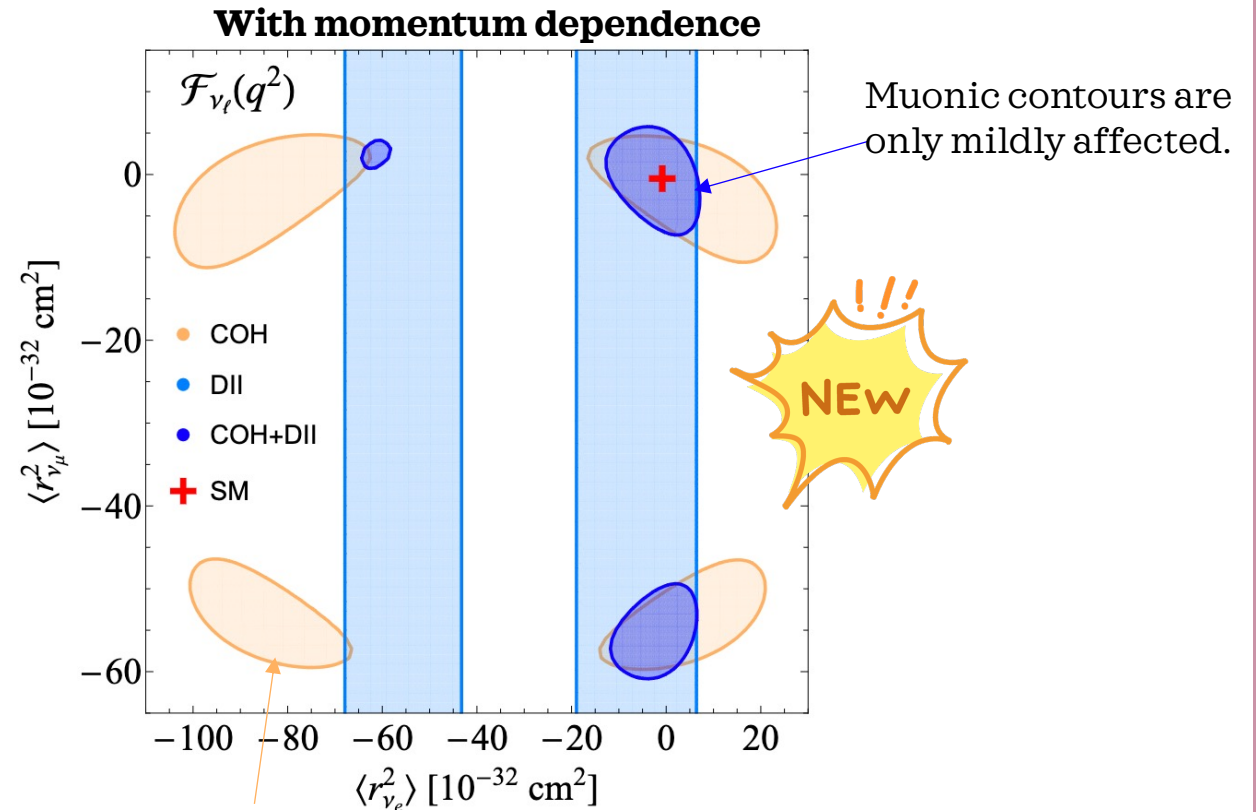
10-20% difference in the proton coupling!

Neutrino charge radius results

- Dataset used: latest COHERENT cesium iodide and argon with the germanium NCC-1701 data (DII).



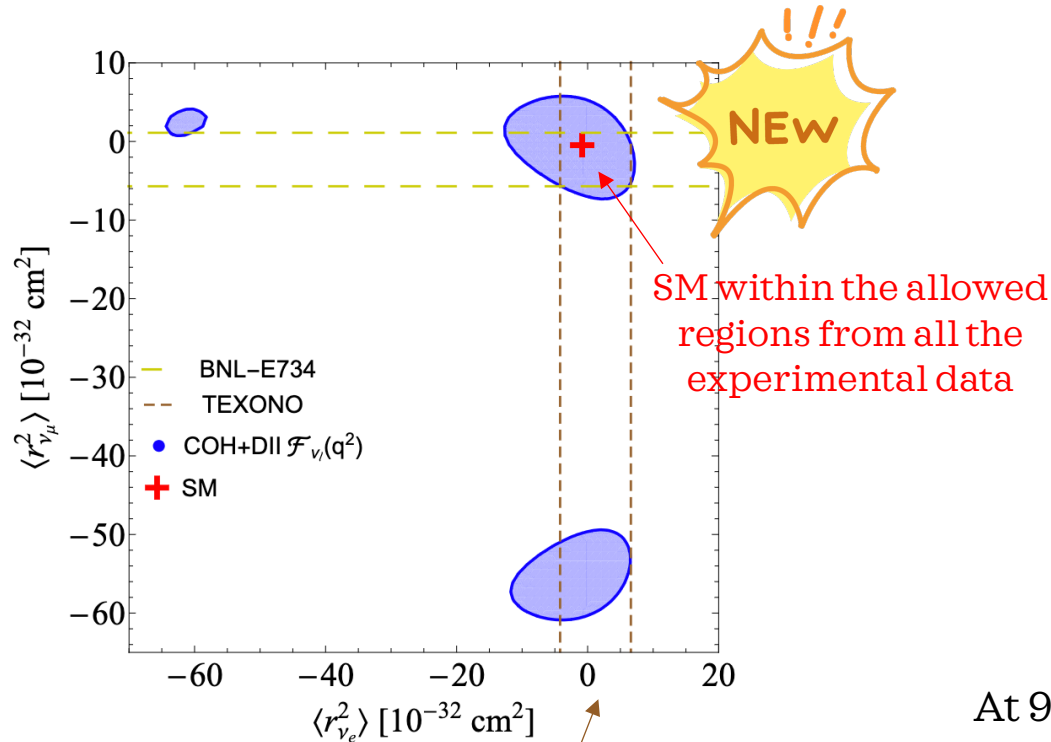
These largely negative values produce a degenerate cross-section



COHERENT results are more affected than reactors due to the larger momentum transfer.

Results

- The main impact of accounting for the NCR form factor is that, by combining the different measurements, the **allowed regions in the parameter space are significantly reduced!**



Current best limits from accelerator $\nu_{e/\mu} - e$ scattering also shown: **TEXONO** $-4.2 < \langle r_{\nu_e}^2 \rangle < 6.6 [10^{-32} \text{ cm}^2]$, **BNL-E734** $-5.7 < \langle r_{\nu_\mu}^2 \rangle < 1.1 [10^{-32} \text{ cm}^2]$ @90% CL

	1σ	90%	2σ	3σ
COHERENT (CsI+Ar)				
$\langle r_{\nu_e}^2 \rangle$	(-95.0, -77.4) (0.09, 12.8)	(-100.0, -69.8) (-8.6, 19.1)	(-102.6, -64.8) (-13.9, 22.2)	(-110.4, 30.7)
$\langle r_{\nu_\mu}^2 \rangle$	(-6.8, 0.5)	(-57.6, -48.9) (-9.3, 2.9)	(-59.2, -47.1) (-10.7, 4.2)	(-63.3, -42.3) (-15.2, 8.1)
Dresden-II				
$\langle r_{\nu_e}^2 \rangle$	(-62.5, -53.7) (-9.0, 1.8)	(-65.7, -48.5) (-13.8, 4.5)	(-67.2, -45.0) (-17.2, 6.0)	(-71.1, 9.7)
COHERENT (CsI+Ar) + Dresden-II				
$\langle r_{\nu_e}^2 \rangle$	(-5.8, 3.1)	(-9.5, 5.5)	(-11.6, 6.8)	(-70.3, -47.7) (-19.8, 10.1)
$\langle r_{\nu_\mu}^2 \rangle$	(-56.8, -53.3) (-4.0, 2.1)	(-59.2, -51.0) (-5.9, 4.1)	(-60.4, -49.9) (-6.9, 5.3)	(-63.8, -46.8) (-9.9, 8.7)

At 90% CL:

$$-9.5 < \langle r_{\nu_e}^2 \rangle [10^{-32} \text{ cm}^2] < 5.5, \text{ Best upper limit!}$$

$$-59.2 < \langle r_{\nu_\mu}^2 \rangle [10^{-32} \text{ cm}^2] < -51.0, \quad -5.9 < \langle r_{\nu_\mu}^2 \rangle [10^{-32} \text{ cm}^2] < 4.1$$



Conclusions

- **Radiative corrections cannot be neglected anymore!**
- Need to **properly account for the non-null momentum transfer of the experiments** in the calculation of the neutrino charge radius radiative correction.
- The systematic bias of the $\nu_e N$ scattering cross section is around 1 -2%, which is an **effect of ~20% with respect to the current systematic uncertainties** affecting CEvNS.
- **For future measurements, it will become imperative to include the momentum dependence!**
- **Mandatory to consider it to extract unbiased charge radii:** moreover it restricts the available phase space.



THANKS FOR YOUR ATTENTION



EPIC 2024

Electroweak Physics Intersections

 22-27 Sept 2024  CalaSerena, Geremeas IT

EPIC 2024 is the first workshop dedicated to **precision electroweak physics**, with focus on:

- Precision tests of the Standard Model and beyond with atomic nuclei
- Lepton- and neutrino-nucleus interactions
- Nuclear matter across energy scales and multi-messenger astronomy

PRE-WORKSHOP SCHOOL

- One-day lectures on precision physics with atoms, neutrino physics, and nuclear EoS in the multimessenger era.
- Dedicated poster session for students at the workshop with teaser-talk event.

SCIENTIFIC PROGRAM COMMITTEE

Sonia Bacca (JGU Mainz)
Matteo Cadeddu (INFN Cagliari)
Nicola Cargioli (INFN Cagliari)
Francesca Dordei (INFN Cagliari)
Mikhail Gorshteyn (JGU Mainz)

EPIC WEBSITE



REGISTER HERE



LOCATION



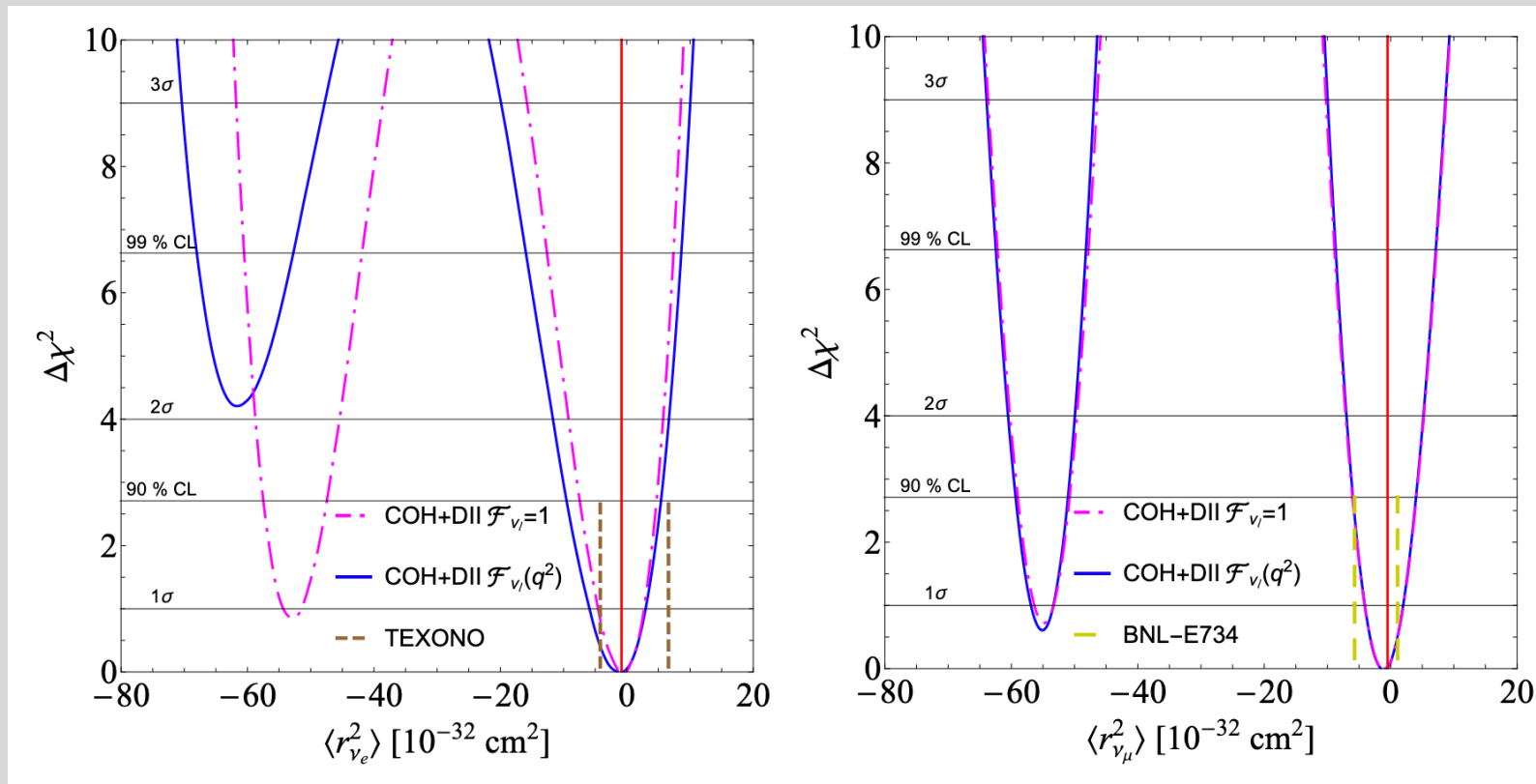
ORGANIZED BY





BACKUP

1D PROJECTIONS



Agreement between the two formalisms

It can be noticed that the difference of the weak mixing angle values consists only of a small constant term:

$$k_{\nu_\ell}(q^2 = 0)\hat{s}_Z^2 - \hat{s}_0^2(\text{RGE}) = -\frac{2\alpha}{9\pi} + \mathcal{O}(\alpha^2)$$

See also Appendix A of arXiv: 2309.04060

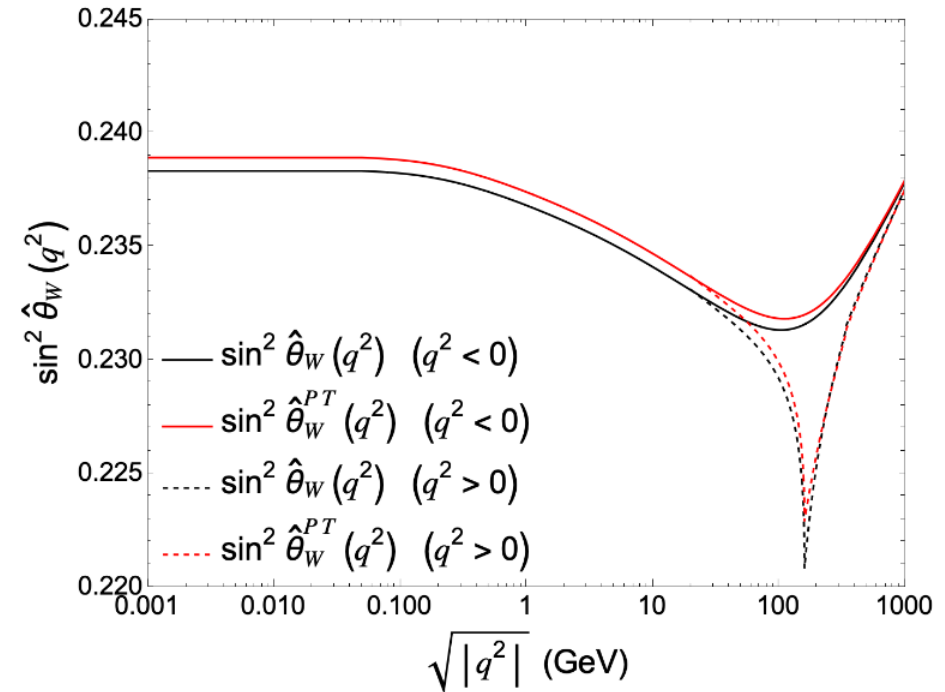
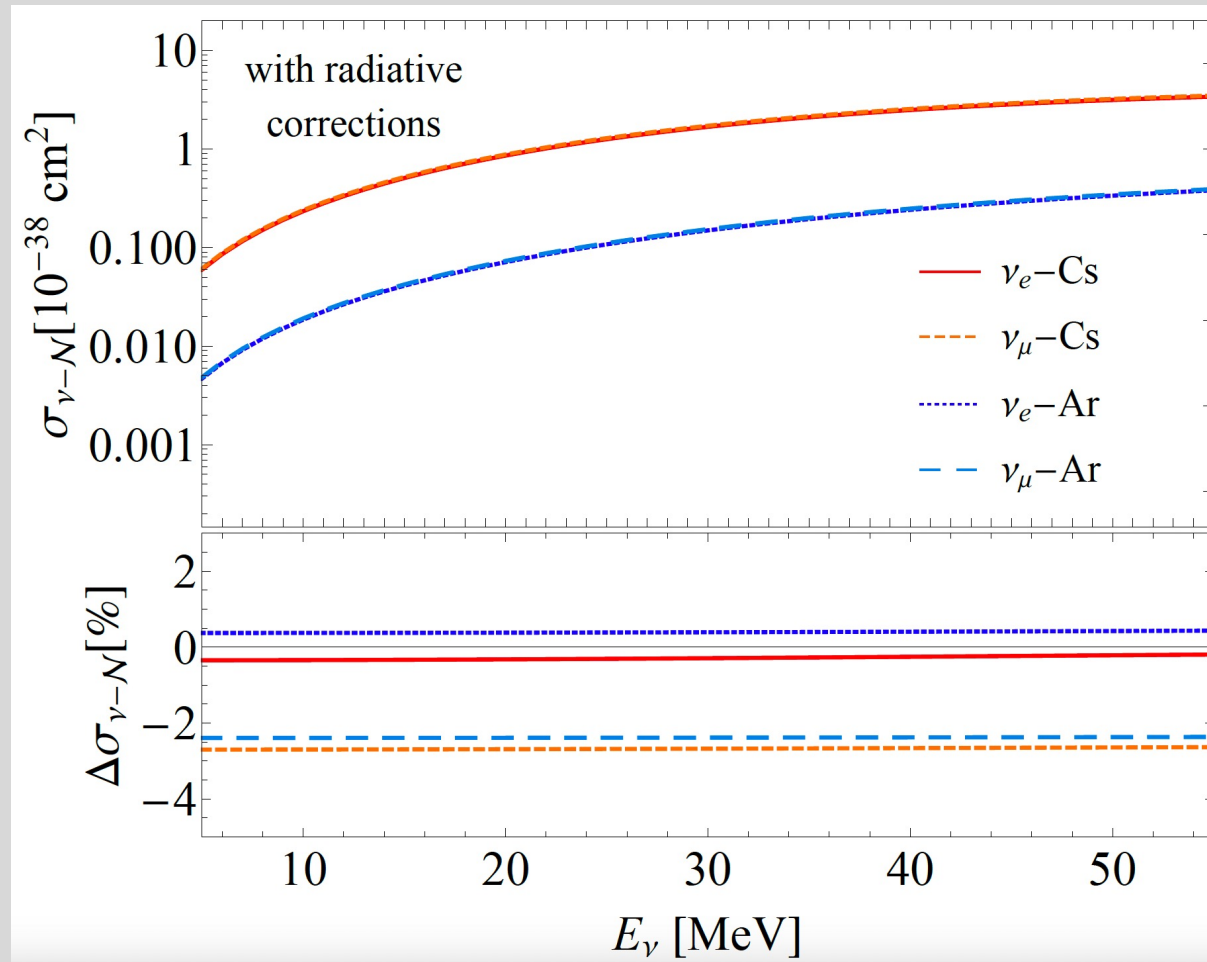


FIG. 9. A comparison of typical form $\sin^2 \hat{\theta}_W(q^2)$ in black and PT form $\sin^2 \hat{\theta}_W^{PT}(q^2)$ in red. Solid (dashed) curves represent spacelike (timelike) momenta. The curves for timelike momenta are shown only in a domain $\sqrt{|q^2|} > 20$ GeV.

Impact of radiative corrections @ $q^2=0$



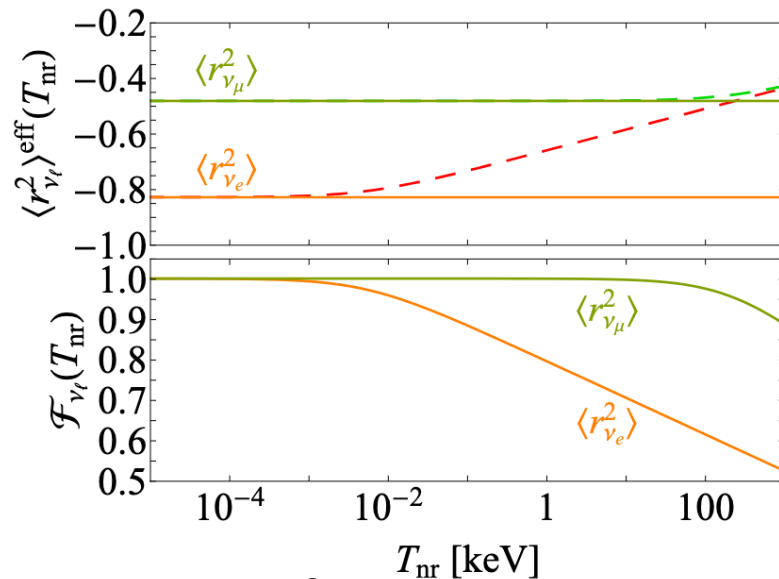
From N. Cargioli PhD's thesis

The effective charge radius form factor

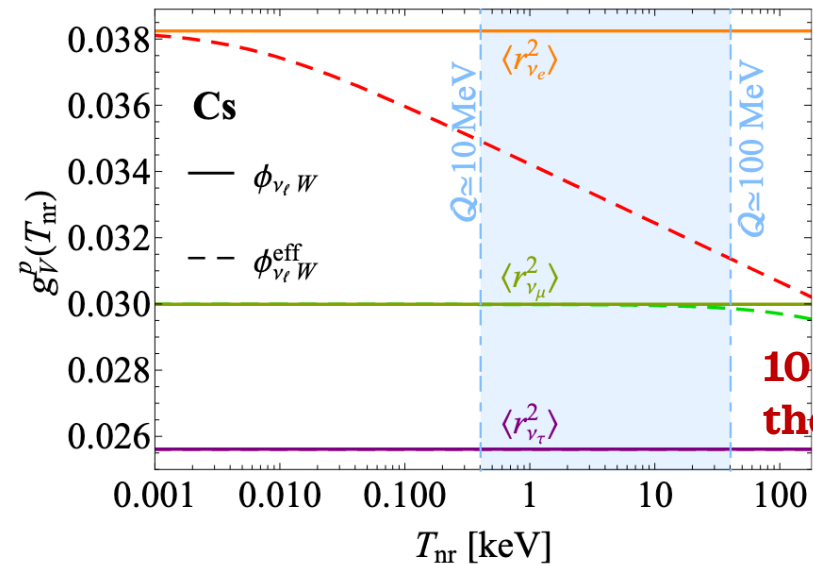
We introduce a **neutrino charge radius form factor** $\mathcal{F}_{\nu_\ell}(T_{\text{nr}}) = \frac{\langle r_{\nu_\ell}^2 \rangle^{\text{eff}}(T_{\text{nr}})}{\langle r_{\nu_\ell}^2 \rangle^{\text{eff}}(0)} \equiv \frac{\langle r_{\nu_\ell}^2 \rangle^{\text{eff}}(T_{\text{nr}})}{\langle r_{\nu_\ell}^2 \rangle^{\text{SM}}}$

with $\langle r_{\nu_\ell}^2 \rangle^{\text{eff}} = \frac{6G_F}{\sqrt{2}\pi\alpha} \phi_{\nu_\ell W}^{\text{eff}}(q^2) = -\frac{G_F}{2\sqrt{2}\pi^2} [3 - 12R_\ell(q^2)]$

From which we obtain an updated proton coupling:



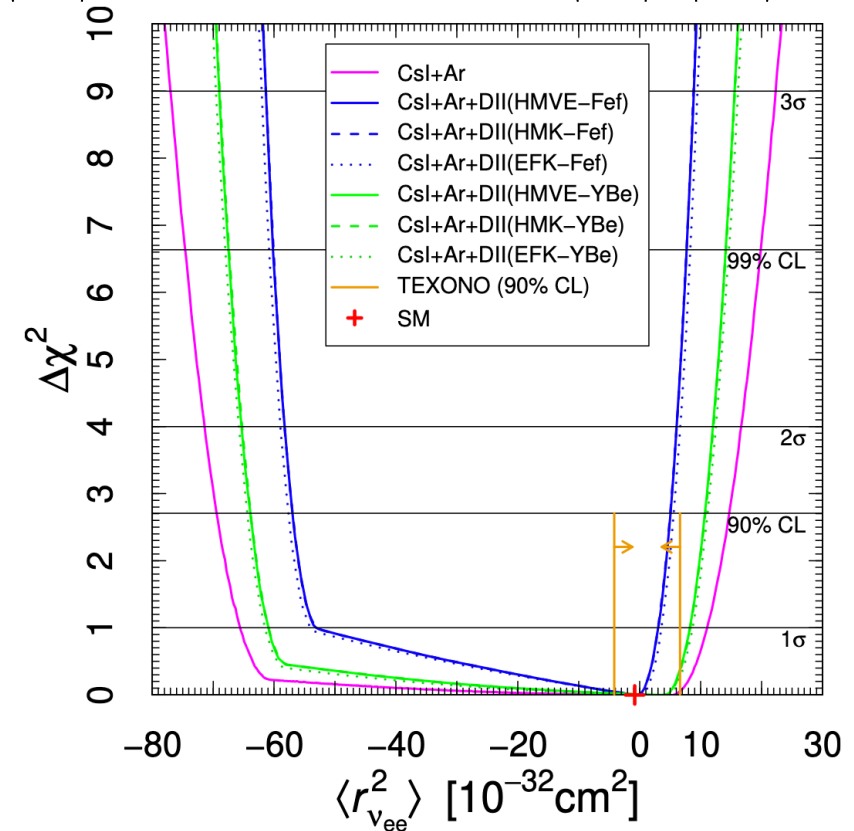
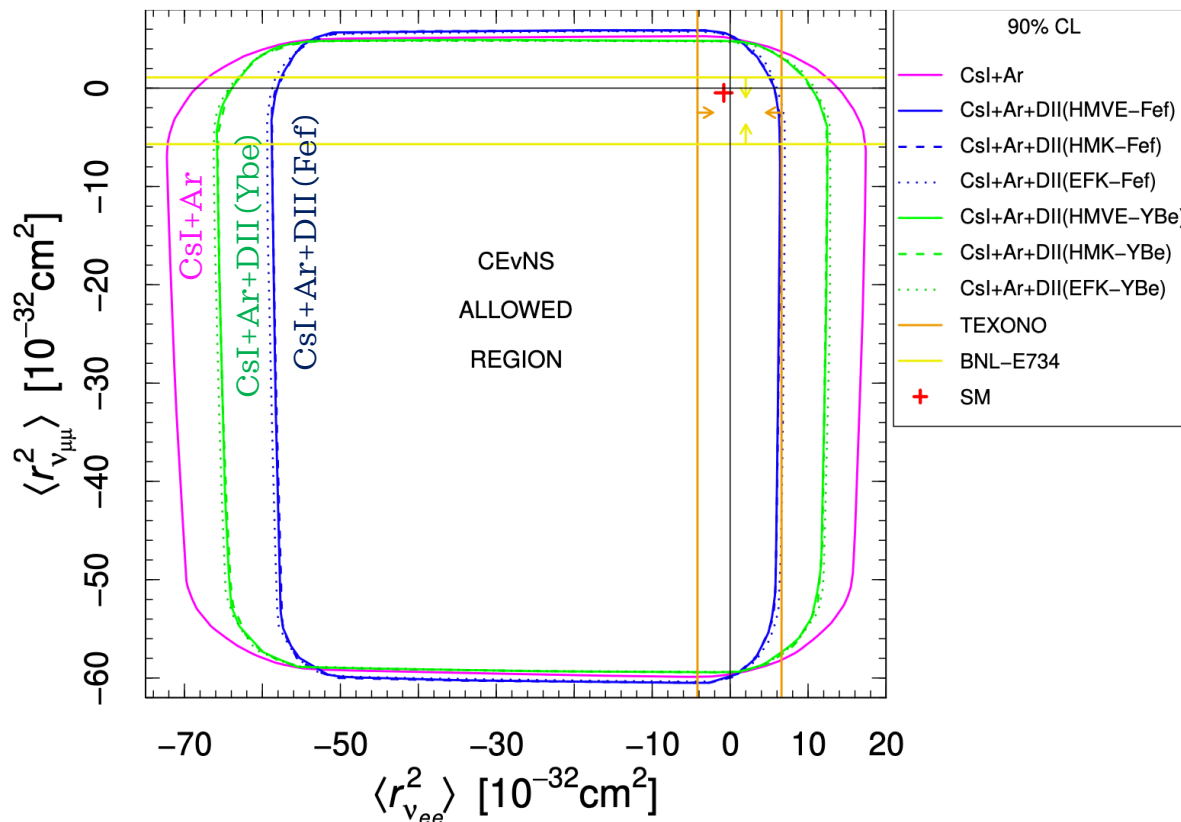
Impact visible for $q^2 \gtrsim m_\ell^2$, for ν_e processes the correction to the couplings becomes visible for $q \gtrsim 0.5$ MeV, while for ν_μ only above ~ 100 MeV!



10-20% difference in the proton coupling!

Neutrino charge radius – previous results

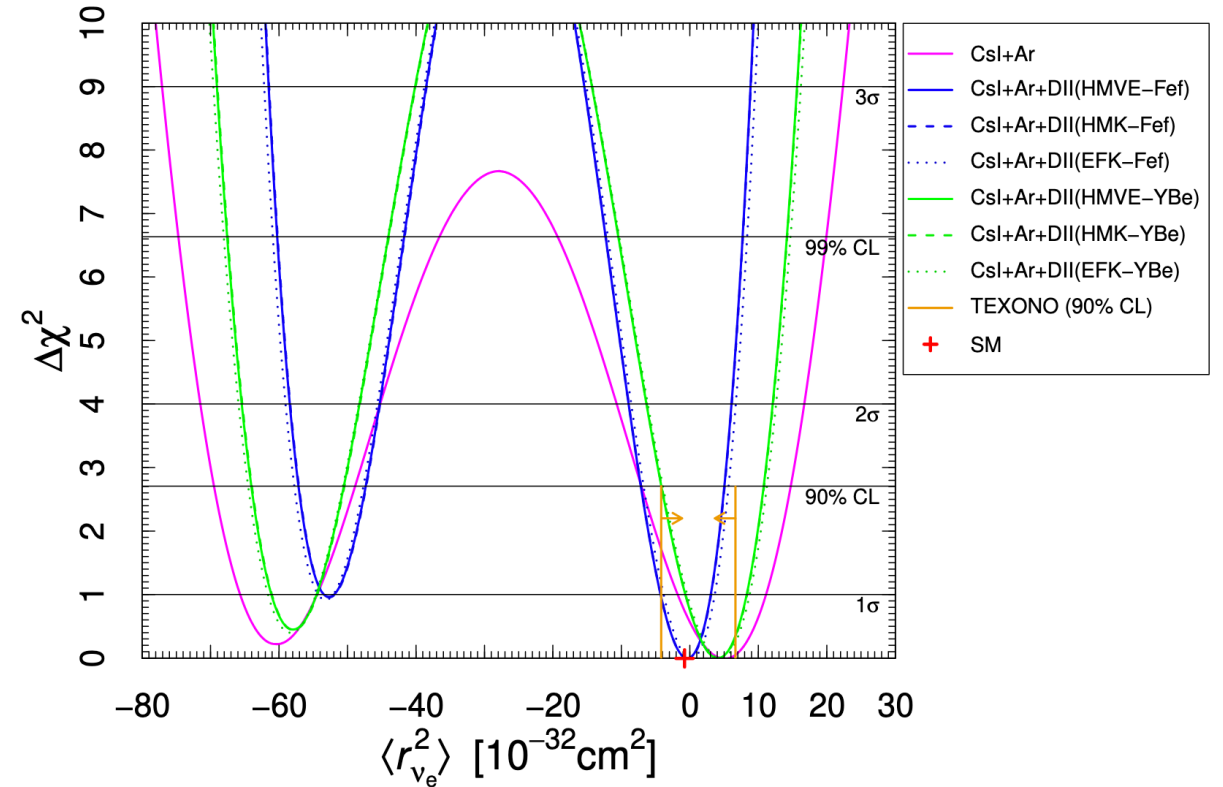
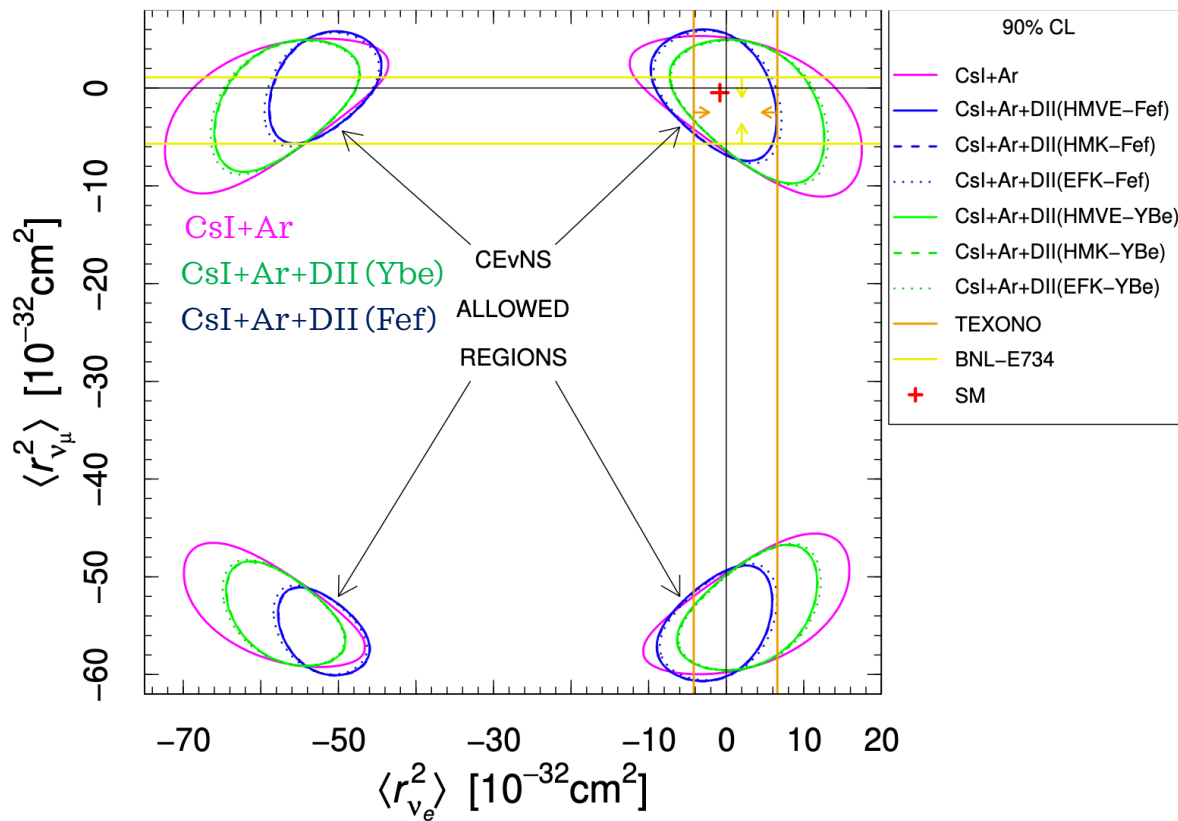
Assuming the **presence of transition CR**, **DRESDEN-II** can measure $\langle r_{\nu_{ee}}^2 \rangle, |\langle r_{\nu_{e\mu}}^2 \rangle|, |\langle r_{\nu_{e\tau}}^2 \rangle|$ **COHERENT** also $|\langle r_{\nu_{\mu\tau}}^2 \rangle|, \langle r_{\nu_{\mu\mu}}^2 \rangle$



- The CsI + Ar COHERENT combination is **vastly dominated by CsI**.
- **Dresden-II** and **CsI** datasets contribute with **roughly same precision**.
- **HMVE, HMK, EFK** different flux parametrization: practically independent, **highly sensitive to the QF used**.

Neutrino charge radius – previous results

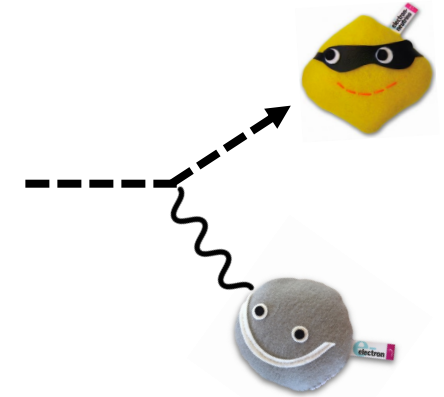
Assuming the **absence of transition CR**: $\langle r_{\nu_e}^2 \rangle \equiv \langle r_{\nu_{ee}}^2 \rangle$ and $\langle r_{\nu_\mu}^2 \rangle \equiv \langle r_{\nu_{\mu\mu}}^2 \rangle$



$-7.1 < \langle r_{\nu_e}^2 \rangle < 5 [10^{-32} \text{cm}^2]$ **COHERENT + DRESDEN-II @ 90% CL**

- When using the Fef QF we **set a better upper bound with respect to that set by TEXONO** ($6.6 \times 10^{-32} \text{cm}^2$)
- **No effect is found due to ES** on the neutrino CR, thus the results are independent of its inclusion

ELASTIC ν – ELECTRON SCATTERING



- ν -electron elastic scattering (ES) is a **concurrent process to CEvNS**
- In the SM, its contribution to the total event rate is small and can be neglected
- **In certain BSM scenarios the ES contribution increases significantly** ➔ Allows us to achieve stronger constraints !

$$\frac{d\sigma^{ES}(E_\nu, T_e)}{dT_e} = Z_{eff}^A(T_e) \frac{G_F^2 m_e}{2\pi} \left[(g_V^{\nu_l} + g_A^{\nu_l})^2 + (g_V^{\nu_l} - g_A^{\nu_l})^2 \left(1 - \frac{T_e}{E_\nu}\right)^2 - ((g_V^{\nu_l})^2 - (g_A^{\nu_l})^2) \frac{m_e T_e}{E_\nu^2} \right] + \text{radiative corrections}$$

Neutrino energy \rightarrow E_ν

Mass of the electron \rightarrow m_e

SM neutrino electron coupling \rightarrow $g_V^{\nu_l}, g_A^{\nu_l}$

Electron recoil energy \rightarrow T_e

The interaction is not with free electrons but atomic electrons!
Quantifies the **number of electrons that can be ionized by a certain energy deposit T_e** .

$g_V^{\nu_e} = 2 \sin^2 \theta_W + 1/2, \quad g_A^{\nu_e} = 1/2,$
 $g_V^{\nu_{\mu,\tau}} = 2 \sin^2 \theta_W - 1/2, \quad g_A^{\nu_{\mu,\tau}} = -1/2$

- The $Z_{eff}^A(T_e)$ term is needed to correct the cross section derived under the Free Electron Approximation (FEA) hypothesis, where electrons are considered to be free and at rest (would just scale as Z).
- Alternative ab-initio approach: **multi-configuration relativistic random phase approximation** (MCRRPA) able to improve the description of the atomic many-body effects
- We do not include such contribution for Ar, where the f_{90} parameter removes electron recoils due to ES

☐ PRA 25 (1982) 634

The Z_{eff} term

$Z_{\text{eff}}^{\text{Cs}} =$	55,	$T_e > 35.99 \text{ keV}$	$Z_{\text{eff}}^{\text{I}} =$	53,	$T_e > 33.17 \text{ keV}$
	53,	$35.99 \text{ keV} \geq T_e > 5.71 \text{ keV}$		51,	$33.17 \text{ keV} \geq T_e > 5.19 \text{ keV}$
	51,	$5.71 \text{ keV} \geq T_e > 5.36 \text{ keV}$		49,	$5.19 \text{ keV} \geq T_e > 4.86 \text{ keV}$
	49,	$5.36 \text{ keV} \geq T_e > 5.01 \text{ keV}$		47,	$4.86 \text{ keV} \geq T_e > 4.56 \text{ keV}$
	45,	$5.01 \text{ keV} \geq T_e > 1.21 \text{ keV}$		43,	$4.56 \text{ keV} \geq T_e > 1.07 \text{ keV}$
	43,	$1.21 \text{ keV} \geq T_e > 1.07 \text{ keV}$		41,	$1.07 \text{ keV} \geq T_e > 0.93 \text{ keV}$
	41,	$1.07 \text{ keV} \geq T_e > 1 \text{ keV}$		39,	$0.93 \text{ keV} \geq T_e > 0.88 \text{ keV}$
	37,	$1 \text{ keV} \geq T_e > 0.74 \text{ keV}$		35,	$0.88 \text{ keV} \geq T_e > 0.63 \text{ keV}$
	33,	$0.74 \text{ keV} \geq T_e > 0.73 \text{ keV}$		31,	$0.63 \text{ keV} \geq T_e > 0.62 \text{ keV}$
	27,	$0.73 \text{ keV} \geq T_e > 0.23 \text{ keV}$		25,	$0.62 \text{ keV} \geq T_e > 0.19 \text{ keV}$
25,	$0.23 \text{ keV} \geq T_e > 0.17 \text{ keV}$	23,	$0.19 \text{ keV} \geq T_e > 0.124 \text{ keV}$		
23,	$0.17 \text{ keV} \geq T_e > 0.16 \text{ keV}$	21,	$0.124 \text{ keV} \geq T_e > 0.123 \text{ keV}$		
19,	$T_e < 0.16 \text{ keV}$	17,	$T_e < 0.123 \text{ keV}$		

Table 1. The effective electron charge of the target atom, $Z_{\text{eff}}^{\text{A}}(T_e)$, for Cs and I.

$Z_{\text{eff}}^{\text{Ge}} =$	32,	$T_e > 11.103 \text{ keV}$
	30,	$11.103 \text{ keV} \geq T_e > 1.4146 \text{ keV}$
	28,	$1.4146 \text{ keV} \geq T_e > 1.2481 \text{ keV}$
	26,	$1.2481 \text{ keV} \geq T_e > 1.217 \text{ keV}$
	22,	$1.217 \text{ keV} \geq T_e > 0.1801 \text{ keV}$
	20,	$0.1801 \text{ keV} \geq T_e > 0.1249 \text{ keV}$
	18,	$0.1249 \text{ keV} \geq T_e > 0.1208 \text{ keV}$
	14,	$0.1208 \text{ keV} \geq T_e > 0.0298 \text{ keV}$
	10,	$0.0298 \text{ keV} \geq T_e > 0.0292 \text{ keV}$
	4,	$T_e \leq 0.0292 \text{ keV}$

Table 2. The effective electron charge of the target atom, $Z_{\text{eff}}^{\text{A}}(T_e)$, for Ge.

Specific for each atom, obtained using edge energies from photo-absorption data.

 A. Thompson et al., X-ray data booklet, <https://xdb.lbl.gov/>, Lawrence Berkeley National Laboratory, U.S.A. (2009)

The charge radii summary

Process	Collaboration	Limit [10^{-32} cm^2]	C.L.	Ref.
Reactor $\bar{\nu}_e$ - e	Krasnoyarsk	$ \langle r_{\nu_e}^2 \rangle < 7.3$	90%	[94]
	TEXONO	$-4.2 < \langle r_{\nu_e}^2 \rangle < 6.6$	90%	[91] ^a
Accelerator ν_e - e	LAMPF	$-7.12 < \langle r_{\nu_e}^2 \rangle < 10.88$	90%	[95] ^a
	LSND	$-5.94 < \langle r_{\nu_e}^2 \rangle < 8.28$	90%	[96] ^a
Accelerator ν_μ - e and $\bar{\nu}_\mu$ - e	BNL-E734	$-5.7 < \langle r_{\nu_\mu}^2 \rangle < 1.1$	90%	[92] ^{a, b}
	CHARM-II	$ \langle r_{\nu_\mu}^2 \rangle < 1.2$	90%	[97] ^a
COHERENT + Dresden-II	w/o transition CR	$-7.1 < \langle r_{\nu_e}^2 \rangle < 5$	90%	This work ^c
	w transition CR	$-56 < \langle r_{\nu_e}^2 \rangle < 5$	90%	This work ^c
COHERENT + Dresden-II	w/o transition CR	$-5.9 < \langle r_{\nu_\mu}^2 \rangle < 4.3$	90%	This work ^c
	w transition CR	$-58.2 < \langle r_{\nu_\mu}^2 \rangle < 4.0$	90%	This work ^c

^aCorrected by a factor of two due to a different convention, see ref. [21].

^bCorrected in ref. [93].

^cUsing the Fef quenching factor.

Table 7. Experimental limits for the neutrino charge radii.